DEVELOPMENTAL DYNAMICS 244:1–9, 2015
DOI: 10.1002/DVDY.24209



RESEARCH ARTICLE

# *carbamoyl-phosphate synthetase 2, aspartate transcarbamylase*, and *dihydroorotase* (*cad*) Regulates Notch Signaling and Vascular Development in Zebrafish

**Baptiste Coxam,[1] Christine Neyt,[1] Daniela R. Grassini,[1] Ludovic Le Guen,[1] Kelly A. Smith,[1] Stefan Schulte-Merker,[2,3] and Benjamin M. Hogan[1]***

[1]Division of Molecular Genetics and Development, Institute for Molecular Bioscience, The University of Queensland, Brisbane, QLD, Australia
[2]Hubrecht Institute –KNAW & UMC Utrecht, Utrecht, The Netherlands
[3]EZO, WUR, Wageningen, The Netherlands

**Background: The interplay between Notch and Vegf signaling regulates angiogenesis in the embryo. Notch signaling limits the responsiveness of endothelial cells to Vegf to control sprouting. Despite the importance of this regulatory relationship, much remains to be understood about extrinsic factors that modulate the pathway. Results: During a forward genetic screen for novel regulators of lymphangiogenesis, we isolated a mutant with reduced lymphatic vessel development. This mutant also exhibited hyperbranching arteries, reminiscent of Notch pathway mutants. Positional cloning identified a missense mutation in the *carbamoyl-phosphate synthetase 2, aspartate transcarbamylase*, and *dihydroorotase* (*cad*) gene. Cad is essential for UDP biosynthesis, which is necessary for protein glycosylation and de novo biosynthesis of pyrimidine-based nucleotides. Using a transgenic reporter of Notch activity, we demonstrate that Notch signaling is significantly reduced in *cad*$^{hu10125}$ mutants. In this context, genetic epistasis showed that increased endothelial cell responsiveness to Vegfc/Vegfr3 signaling drives excessive artery branching. Conclusions: These findings suggest important posttranslational modifications requiring Cad as an unappreciated mechanism that regulates Notch/Vegf signaling during angiogenesis. *Developmental Dynamics 244:1–9, 2015*. © 2014 Wiley Periodicals, Inc.**

**Key words:** zebrafish; Notch; Vegfc; glycosylation; angiogenesis; lymphangiogenesis

Submitted 14 July 2014; First Decision 19 September 2014; Accepted 22 September 2014; Published online 7 October 2014

## Introduction

In the developing embryo, angiogenesis is a complex process requiring precise and timely interplay of multiple signaling pathways and cellular processes. Blood vessels arise from preexisting vessels in a spatio-temporally regulated process involving the sprouting, migration, proliferation and patterning of endothelial cells into mature, functional, vessel networks (Herbert and Stainier, 2011). Distinct signaling pathways regulate the formation of arteries and veins and both express a unique combination of markers that reflects vessel function (Adams and Alitalo, 2007).

In the zebrafish, the formation of the initial artery-derived intersegmental vessel network occurs from the dorsal aorta (DA). This process is termed primary angiogenesis and involves the dorsal sprouting of a wave of endothelial cells from the DA to give rise to arterial intersegmental vessels (aISVs) from 19 hr postfertilization (hpf) (Isogai et al., 2003). From 32 hpf, endothelial cells emerge from the posterior cardinal vein (PCV), in a process termed secondary angiogenesis to form intersegmental veins (vISVs) and lymphatic vascular precursor cells which migrate to the horizontal myoseptum where they are known as parachordal lymphangioblasts (PLs) (Isogai et al., 2003; Hogan et al., 2009a; Koltowska et al., 2013).

A large number of studies have shown that zebrafish primary angiogenesis is regulated by Vegfa mediated signaling through the receptors Kdrl and Kdr (Nasevicius et al., 2000; Habeck et al., 2002; Covassin et al., 2006; Bahary et al., 2007). The Notch signaling pathway suppresses Vegf-mediated signaling to limit sprouting during primary angiogenesis (Siekmann and Lawson, 2007). As such, inhibition of Notch signaling in mutants, morphants, or using chemical inhibitors in vivo results in abnormal sprouting of arterial endothelial cells and embryos present with hyperbranching aISVs (Lawson et al., 2001; Lawson and Weinstein, 2002; Leslie et al., 2007; Geudens et al., 2010). These hyperbranching phenotypes can be rescued by loss of Vegfc or Vegfr3 (Siekmann and Lawson, 2007; Hogan et al., 2009b; Villefranc et al., 2013).

Additional Supporting Information may be found in the online version of this article.
Grant sponsor: ARC Future Fellowships; Grant number: FT100100165; Grant number: FT110100496; Grant sponsor: NHMRC; Grant number: 1050138.
Drs. Coxam and Neyt contributed equally to this work.
*Correspondence to: Ben Hogan, Division of Molecular Genetics and Development, Institute for Molecular Bioscience, University of Queensland, St Lucia, 4072 QLD, Australia. E-mail: b.hogan@imb.uq.edu.au

Article is online at: http://onlinelibrary.wiley.com/doi/10.1002/dvdy.24209/abstract

The many developmental roles of Notch signaling rely upon several modulatory pathways to determine context-dependent activity (Guruharsha et al., 2012). A subset of modulators act on Notch signaling through receptor and ligand posttranslational modifications, particularly ubiquitination and glycosylation (Haines and Irvine, 2003; Kovall and Blacklow, 2010). Such modulators include the well described ubiquitin-ligases *mindbomb* and *neuralized* (Yeh et al., 2001; Itoh et al., 2003) and the glycosyltransferase Fringe (Blair, 2000). Although studies have demonstrated the importance of *mindbomb*-mediated ubiquitination during zebrafish angiogenesis (Lawson et al., 2001; Lawson and Weinstein, 2002), little is known about the roles of other post-translational modifications, including glycosylation.

This study presents a zebrafish mutant identified due to a reduction in the development of lymphatic vessels that also displays hyperbranching of intersegmental vessels. We find that the causative mutation occurs in the *carbamoyl-phosphate synthetase 2, aspartate transcarbamylase*, and *dihydroorotase* (*cad*) gene. Our findings show that this gene modulates Notch signaling. Given the known role of Cad in UDP biosynthesis, upstream of glycosylation events, we suggest that it likely acts during post-translational glycosylation in the Notch pathway. This study identifies an unappreciated level of regulation in zebrafish vascular development and identifies the UDP-biosynthesis pathway as a potential target to modulate Notch activity in vivo.

## Results

### *hu10125* Mutants Display Reduced Formation of the Thoracic Duct and Hyperbranched Intersegmental Arteries

During a forward genetic screen for novel zebrafish lymphatic mutants, we isolated a mutant designated *hu10125*. This mutant presented with a significant disruption in the formation of the thoracic duct at 4 days post fertilization (dpf) (Fig. 1A,B, asterisks, I). We also observed hyperbranching of the aISVs in these mutants (Fig. 1A,B,E,F, I) and increased formation of PLs in mutant embryos (Fig. 1I). This phenotype was progressive with 30 hpf ISVs appearing to be normal in mutants (Fig. 1C,D). The *hu10125* vascular defects were also associated with notable morphological defects in nonvascular tissues, including a smaller head and eyes from 2 dpf onward and an atrophied lower jaw (e.g., Fig. 2F), but not with any visible circulatory defects in the trunk at 4 dpf (Supplementary movies 1 and 2).

To address the nature of hyperbranching in *hu10125* mutants, we took advantage of a transgenic line *Tg*(*flt1:tomato*) labeling the arterial vasculature. Phenotypic analysis in this line demonstrated that the hyperbranching phenotype affects the aISVs (Fig. 1E,F). We subsequently set out to investigate whether the arterial hyperbranching was a consequence of excessive proliferation of aISV endothelial cells. Using a nuclear vascular endothelial reporter (*fli1:nucEGFP*), we found that endothelial cell number dorsal to the horizontal myoseptum was increased at 3 dpf in mutants compared with controls, consistent with increased aISV proliferation (Fig. 1G–I).

### A Mutation in the *carbamoyl-phosphate synthetase 2, aspartate transcarbamylase*, and *dihydroorotase* (*cad*) Gene Is Responsible for the *hu10125* Phenotype

To characterize the mutated gene responsible for the phenotype, traditional meiotic mapping was used to localize the genetic lesion to a large region (6 Mb) on chromosome 20 (Fig. 2A). This region contained the gene *cad*, for which the previously characterized mutant *perplexed* had been described as displaying a strikingly similar morphology to *hu10125* (Willer et al., 2005). Sequencing of *cad* identified a mutation substituting a conserved residue in the linker region of the Cad protein (Fig. 2B–E). To test whether the *hu10125* mutant is allelic to *perplexed*, we generated compound heterozygotes in a classical complementation assay and observed that 22.5% of the embryos (n = 165) exhibited the mutant phenotype at both the level of gross morphology and vascular hyperbranching (Fig. 2F,G). This confirms the identity of the mutated gene and we hereafter refer to *hu10125* as $cad^{hu10125}$.

Cad is a rate-limiting enzyme required for the formation of UDP sugar, upstream of two different metabolic pathways; the de novo biosynthesis of pyrimidine and pyrimide-based nucleotides (Jones, 1980), and the formation of UDP sugar intermediates, required for UDP-dependent glycosylation events (Haines and Irvine, 2003). Of interest, given the ubiquitous nature of UDP function, in situ hybridization analysis of *cad* gene expression during development showed highly regulated gene expression, including in cells located in positions consistent with the location of developing endothelial cells (ECs) (Fig. 2H–J). To investigate further if Cad is indeed expressed in ECs, we used qPCR for *cad* transcripts in cDNA isolated from FAC sorted populations of arterial endothelial cells. We have previously published data using the same FACs populations, the identity of which was verified using known markers of arteries, veins and lymphatics (Coxam et al., 2014; Kartopawiro et al., 2014). Analysis of cDNA from arterial endothelial cells isolated at 36 and 60 hpf, showed *cad* expression at levels similar to endothelial markers *kdrl*, *flt1*, and *dll4* (Fig. 2J,K). These cells did not express nonendothelial markers *ccbe1* (Fig. 2K) or *pkd1b* (data not shown). Hence these data demonstrate that *cad* is expressed in arterial endothelium and has the potential to play an autonomous role.

### Knockdown of Vegfc/Vegfr3 Signaling Rescues the $cad^{hu10125}$ Artery Hyperbranching Phenotype

Intersegmental vessel hyperbranching such as that observed in $cad^{hu10125}$ mutants, has been previously associated with reduced Notch signaling and subsequently increased Vegfc/Vegfr3 signaling in zebrafish (Hogan et al., 2009b). Morpholino knockdown of *dll4* leads to aISV hyperbranching, which can be rescued (at least in part) by the depletion or mutation of Vegfc or the injection of a soluble, truncated form of Vegfr3 that acts as a ligand trap (Siekmann and Lawson, 2007; Hogan et al., 2009b; Villefranc et al., 2013). These findings revealed that during normal angiogenesis the arterial response to Vegfc/Vegfr3 signaling is suppressed by Dll4/Notch signaling.

We reasoned that if the $cad^{hu10125}$ mutant phenotype was due to perturbed activity of the Notch pathway, the inhibition of Vegfc/Vegfr3 signaling would rescue the $cad^{hu10125}$ phenotype. To test this, we injected morpholino oligomers targeting, *vegfr3* (*flt4*), *vegfc and ccbe1* (a regulator of Vegfc maturation; Jeltsch et al., 2014; Le Guen et al., 2014) into embryos from incrosses of heterozygous $cad^{hu10125}$ carriers. We observed a significant and quantifiable rescue of the aISV hyperbranching phenotype in *cad/MO-ccbe1* and *cad/MO-vegfc* and *cad/MO-vegfr3* embryos (Fig. 3A–F).

It should be noted that Vegfc/Vegfr3 signaling normally plays no role in aISV formation, with validated mutants in this

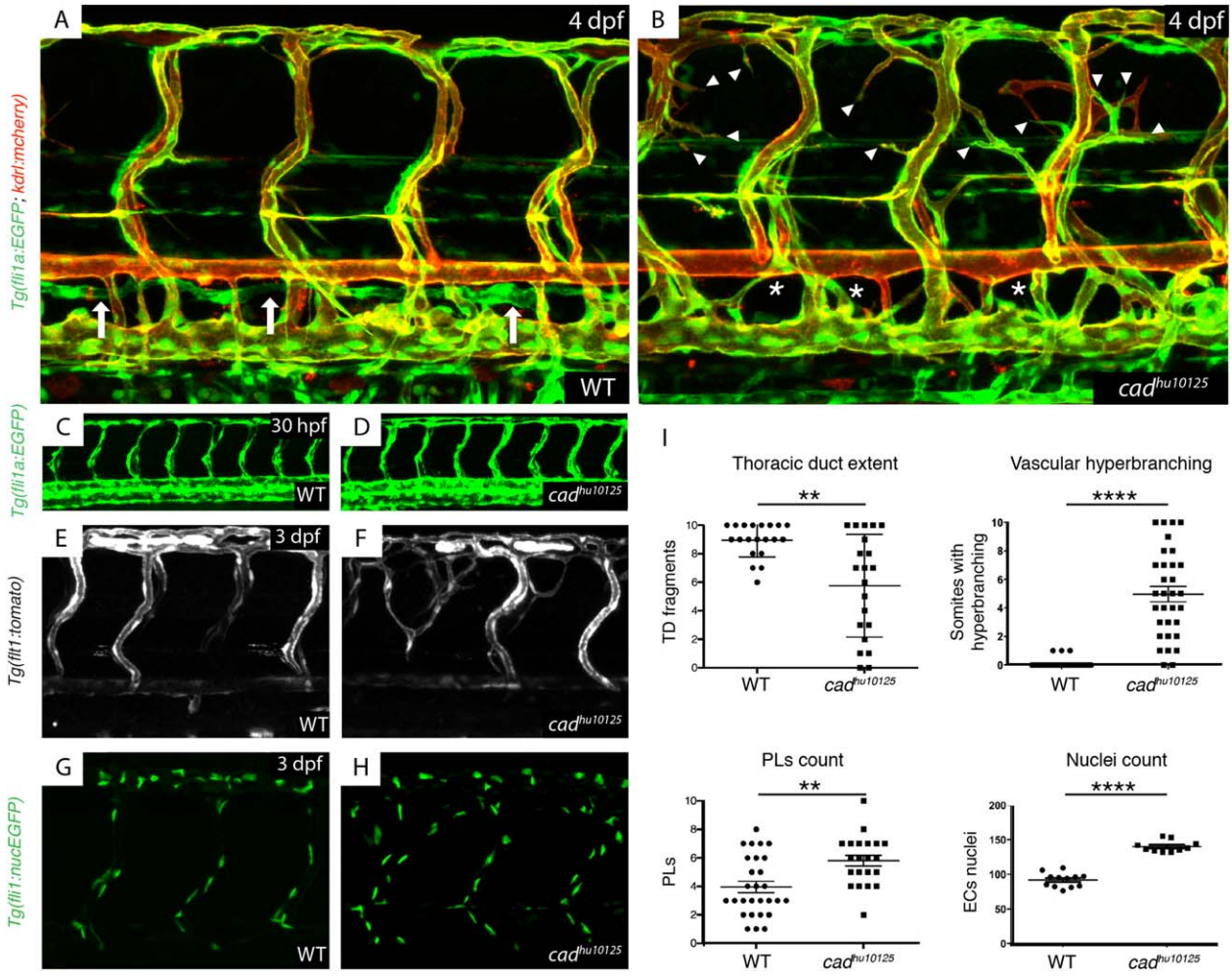


**Fig. 1.** *hu10125* mutants present with lymphatic vascular deficiency and arterial hyperbranching. **A,B:** The vasculature *Tg(fli1a:EGFP; flt1:tomato)* in wild-type siblings (A) and *hu10125* embryos (B) at 4 dpf (white arrows indicate a thoracic duct, asterisk an absence of thoracic duct, and arrowheads indicate hyperbranching). **C,D:** The vasculature *Tg(fli1a:EGFP; flt1:tomato)* in wild-type siblings (n = 53) (C) and *hu10125* (n = 12) embryos (D) at 30 hpf. **E,F:** The arteries *Tg(flt1:tomato)* in wild-type siblings (C) and *hu10125* (D) embryos at 3 dpf. **G,H:** Endothelial nuclei *Tg(fli1:nucEGFP)* in wild-type siblings (G) and *hu10125* (H) embryos at 3 dpf. **I:** Quantification of: thoracic duct extent (number of thoracic duct fragments visible across 10 segments in the trunk) in WT (n = 20) and *hu10125* (n = 21) (4 dpf); vascular hyperbranching (number of bilateral paired ISVs presenting with extra branches across 10 segments in the trunk) in WT (n = 32) and *hu10125* (n = 32) (4 dpf); parachordal lymphangioblasts (number of PLs visible at the level of the horizontal myoseptum, across 10 segments in the trunk) in WT (n = 28) and *hu10125* (n = 21) (56 hpf); and nuclei count (in ISVs, scored dorsal to the horizontal myoseptum across 10 segments) in WT (n = 12) and *hu10125* (n = 10) embryos (3 dpf).

pathway failing to display aISV phenotypes except in genetically sensitized backgrounds (Hogan et al., 2009b; Villefranc et al., 2013; Le Guen et al., 2014). Hence, the rescue observed here is not additive in nature. *cad*$^{hu10125}$ mutant embryos likewise fail to exhibit defects during early angiogenesis (Fig. 1C,D).

## Notch Signaling is Reduced in *cad*$^{hu10125}$ Mutants

Cad regulates the biosynthesis of UDP and hence both thymidine levels and protein glycosylation. Extensive research has demonstrated the importance of posttranslational glycosylation of the Notch receptor on its activity (Haines and Irvine, 2003). This raises the intriguing possibility that Cad may mediate Notch function by means of glycosylation in the context of zebrafish developmental angiogenesis. In support of this hypothesis, we examined the vascular phenotype of the mutant *tyms*$^{hi3510Tg}$, a thymidylate synthase mutant (Amsterdam et al., 2004), affecting the synthesis of de novo thymidine nucleotide from UDP, downstream of Cad and independent of UDP-dependent glycosylation. At 5 dpf, *tyms*$^{hi3510Tg}$ present with a reduction in the size of their head and eyes, phenocopying the eye defects in *cad*$^{hu10125}$ as previously described (Willer et al., 2005) but these mutants do not present with aISV hyperbranching at 4 dpf (Fig. 3G,H). This finding suggests that the vascular phenotype is not due to thymidine synthesis defects, while the eye phenotype most likely is.

To determine if Notch signaling is perturbed in *cad*$^{hu10125}$ mutants, we examined *Tg(Tp1-MmHbb:EGFP)* transgene expression, in which a Notch-responsive promoter (Tp1) drives the expression of EGFP. This strain was examined in *cad*$^{hu10125}$ mutants together with *Tg(flt1:Tomato)* which expresses Tomato selectively in aISVs. We observed strong down regulation of Notch activity throughout the whole embryo in *cad*$^{hu10125}$ mutants (Fig. 4J). In particular, a strong reduction was observed in the neural tube (Fig. 4A–D). The broad embryonic reduction in

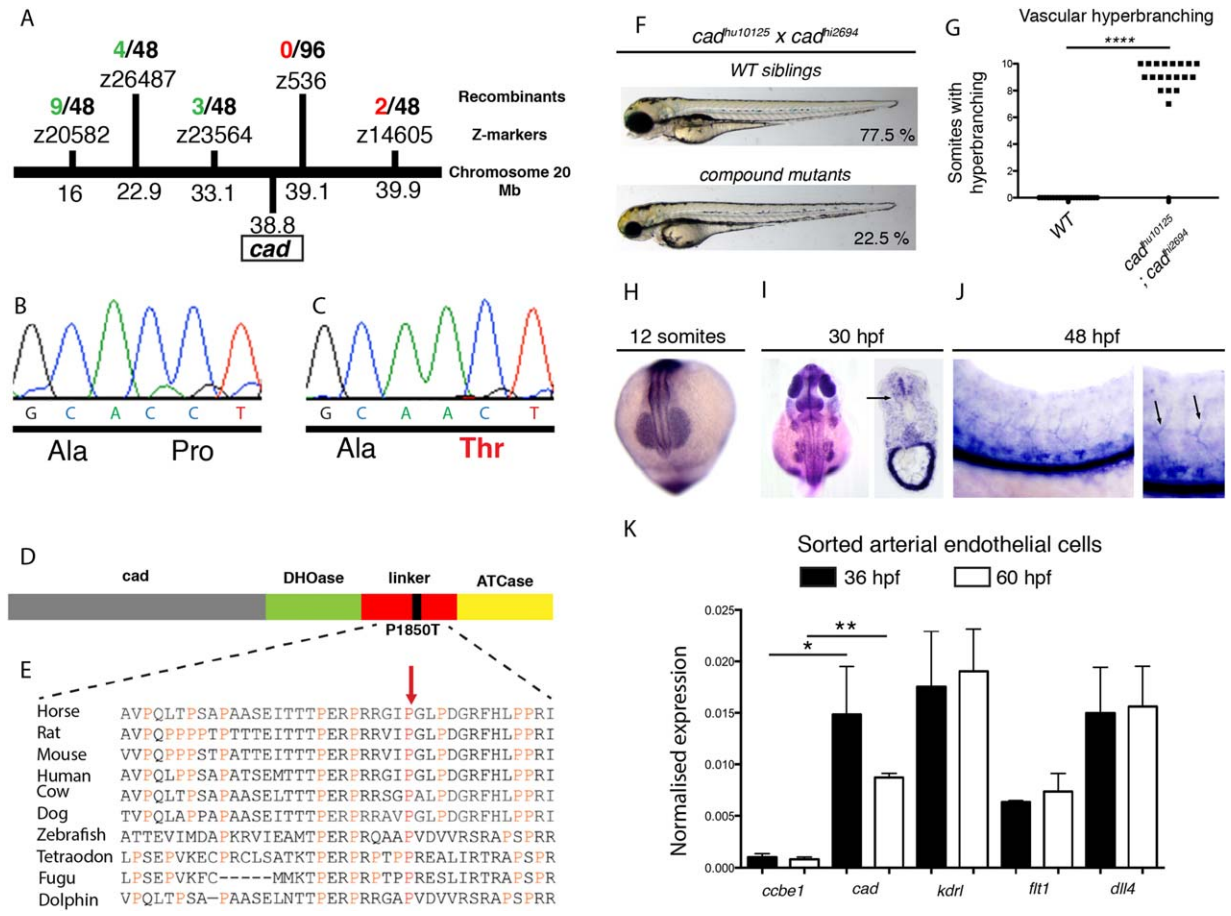


**Fig. 2.** *hu10125* is a *cad (perplexed)* mutant. **A–E:** Overview of the genetic mapping of *cad*$^{hu10125}$ mutants. Recombinant embryos at multiple simple sequence length polymorphism markers identified the critical genetic interval indicated (A). Sequencing of the *cad* gene identified the presence of a mutation (P1850T) in *hu10125* cDNA (B,C), affecting a conserved residue in the linker region of Cad (D,E). **F,G:** Overall morphology of wild-type siblings (77.5 % of the progeny) and *cad*$^{hu10125}$; *cad*$^{hi2694}$ embryos (22.5% of the progeny) at 4 dpf in a classical complementation assay (n = 165 embryos scored) (F). Quantification of the number of intersegmental arteries per embryo (out of 10 segments) presenting with hyperbranching in WT siblings (n = 21 scored) and *cad*$^{hu10125}$;*cad*$^{hi2694}$ (n = 19 scored) embryos at 4 dpf (G). **H–J:** In situ hybridization analysis of *cad* expression shows ubiquitous expression at the 12-somite stage (H), enrichment in the trunk and neural tissues 30 hpf (I) and enrichment within kidney and putative vascular tissues at 48 hpf (J). Arrows: putative vascular endothelial cells. **K:** Quantitative RT-PCR for markers of the blood vasculature in arterial endothelial cells (AECs) sorted based on *TG(flt1:YFP)* expression at 36 and 60 hpf: *kdrl* (expressed in all blood vascular endothelial cells), *flt1* and *dll4* (restricted to arterial endothelial cells), *ccbe1* (not expressed in the vascular endothelium) and *cad*. Gene expression were normalised to *rpl13*.

Notch activity was confirmed by Western blot detection of EGFP expression in *Tg(Tp1-MmHbb:EGFP)* expressing mutant embryos (Fig. 4J) and qPCR for Notch targets *efnb2a* and *hey1* at 3 and 5 dpf. Furthermore, the arterial expression of *Tg(Tp1-MmHbb:EGFP)* in mutant arteries was visualized by limiting analysis in the *Tg(Tp1-MmHbb:EGFP)* strain to cells expressing *Tg(flt1:Tomato)*. In aISVs, we observed a significant reduction in signal, as quantified by EGFP signal intensity relative to average WT intensity (Fig. 4E–I). Overall, these observations demonstrate that Cad is needed for Notch signaling in the developing embryo including in aISVs.

## Discussion

This study identifies an unappreciated modulator of the Notch signaling pathway in zebrafish development. Cad is essential for normal artery development at 3 and 5 dpf and for the formation of the lymphatic vasculature. This mutant was initially isolated for the lymphatic vessel defect. However, it seems likely that this phenotype may be secondary to abnormal artery formation, particularly as the number of lymphatic precursor cells is initially increased and the thoracic duct deficiency highly variable. We demonstrate that the hyperbranching phenotype observed in *cad*$^{hu10125}$ mutant embryos results from increased artery VegfC signaling. We suggest that a down-regulation of Notch activity, which suppresses the response of arteries to signaling through Vegfr3, is the underlying cause for this vascular phenotype. Indeed, *cad*$^{hu10125}$ mutant embryos exhibit a reduction of Notch signaling activity observed in the Notch activity reporter line *Tg(Tp1-MmHbb:EGFP)*. We found reduced expression of Notch target genes and also reduced EGFP in *Tg(Tp1-MmHbb:EGFP)* by Western blot. The difference in the expression of Notch target genes comparing DAPT-treated embryos and *cad*$^{hu10125}$ mutant embryos may reflect that Cad represents a partial loss of Notch scenario, or only influences some receptor or ligand activities. These observations are consistent with an embryo-wide reduction in Notch signaling in both endothelial and nonendothelial tissues as both EGFP and the marker genes used are expressed more

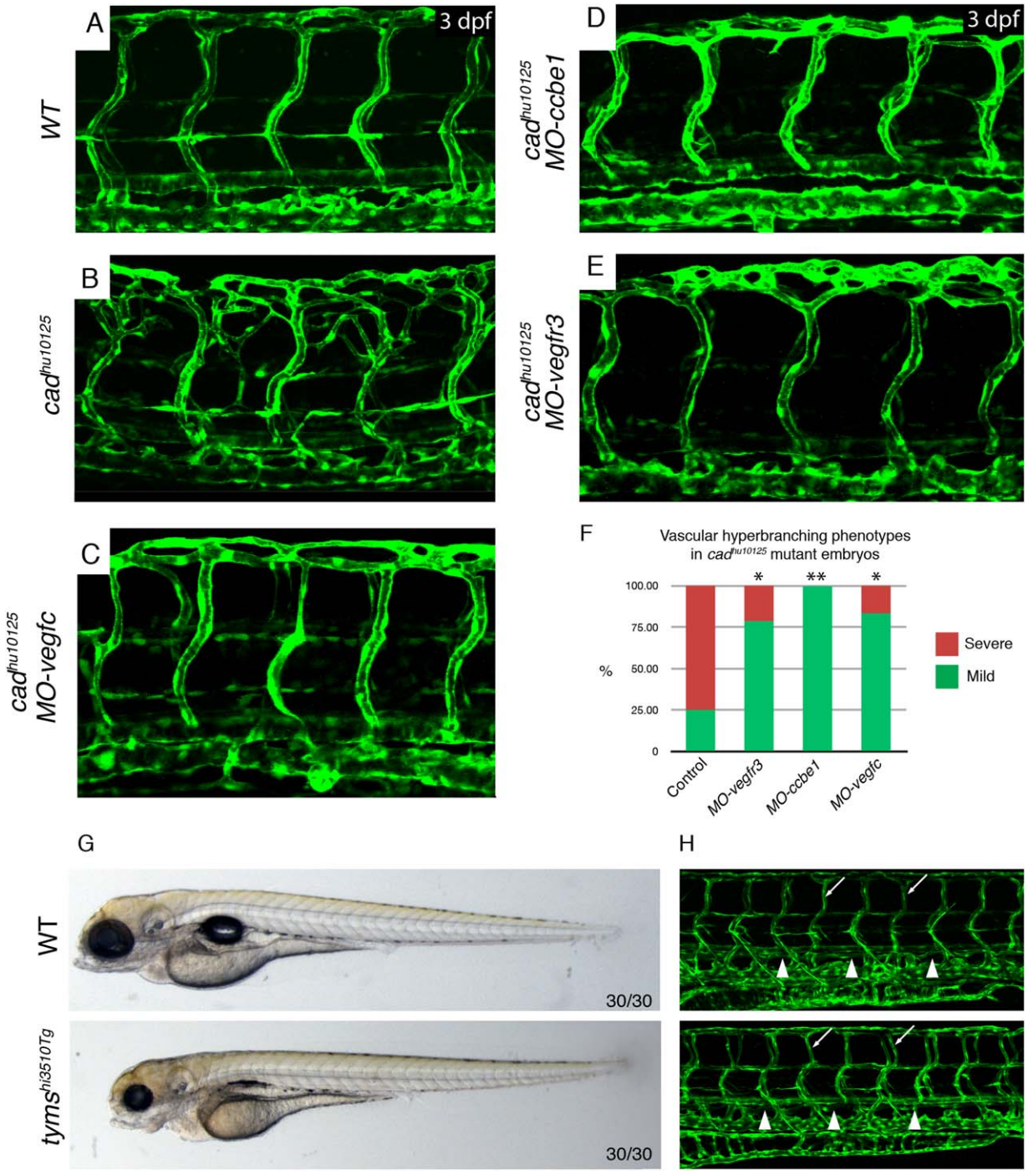


**Fig. 3.** *cad* artery hyperbranching is Vegfc/Vegfr3 dependent. **A,B:** The vasculature *Tg(fli1a:EGFP)* in wild-type sibling (A) and *cad*$^{hu10125}$ (B) embryos at 3 dpf. **C–E:** The vasculature *Tg(fli1a:EGFP)* in *cad*$^{hu10125}$/*MO-vegfc* (C), *cad*$^{hu10125}$/*MO-ccbe1* (D), and *cad*$^{hu10125}$/*MO-vegfr3* (E) embryos at 3 dpf. **F:** Quantification of the severity of vascular hyperbranching designated as mild or severe (where mild: 1–7 hyperbranched arteries, and severe: $\geq$8 hyperbranched arteries along the entire embryo body axis) scored in WT (n = 16), *MO-vegfc* (n = 12), *MO-ccbe1* (n = 10) and *MO-vegfr3* (n = 14) injected *cad*$^{hu10125}$ embryos. **G,H:** The thymidylate synthase mutant *tyms*$^{hi3510Tg}$ does not present with arterial hyperbranching. G: Overall morphology of wild-type (n = 30/30) and t*yms*$^{hi3510Tg}$ (n = 30/30) embryos at 4 dpf. H: The vasculature *Tg(fli1a:EGFP)* in wild-type (n = 30/30) and *tyms*$^{hi3510Tg}$ (n = 30/30) embryos at 4dpf. White arrowhead: thoracic duct, white arrow: example of normal aISV.

widely than just endothelium. The reduction includes a quantifiable reduction in aISVs themselves, which is consistent with the hyperbranching phenotype in these cells and suggests an autonomous reduction in Notch signaling as the mechanism underpinning the phenotype.

We have observed that vascular development proceeds normally in *tyms*$^{hi3510Tg}$ mutants, arguing that the Thymidine nucleotide branch of UDP metabolism is probably not responsible for the vascular phenotype observed in *cad*$^{hu10125}$ mutants. A role for glycosylation in the function of the Notch pathway is

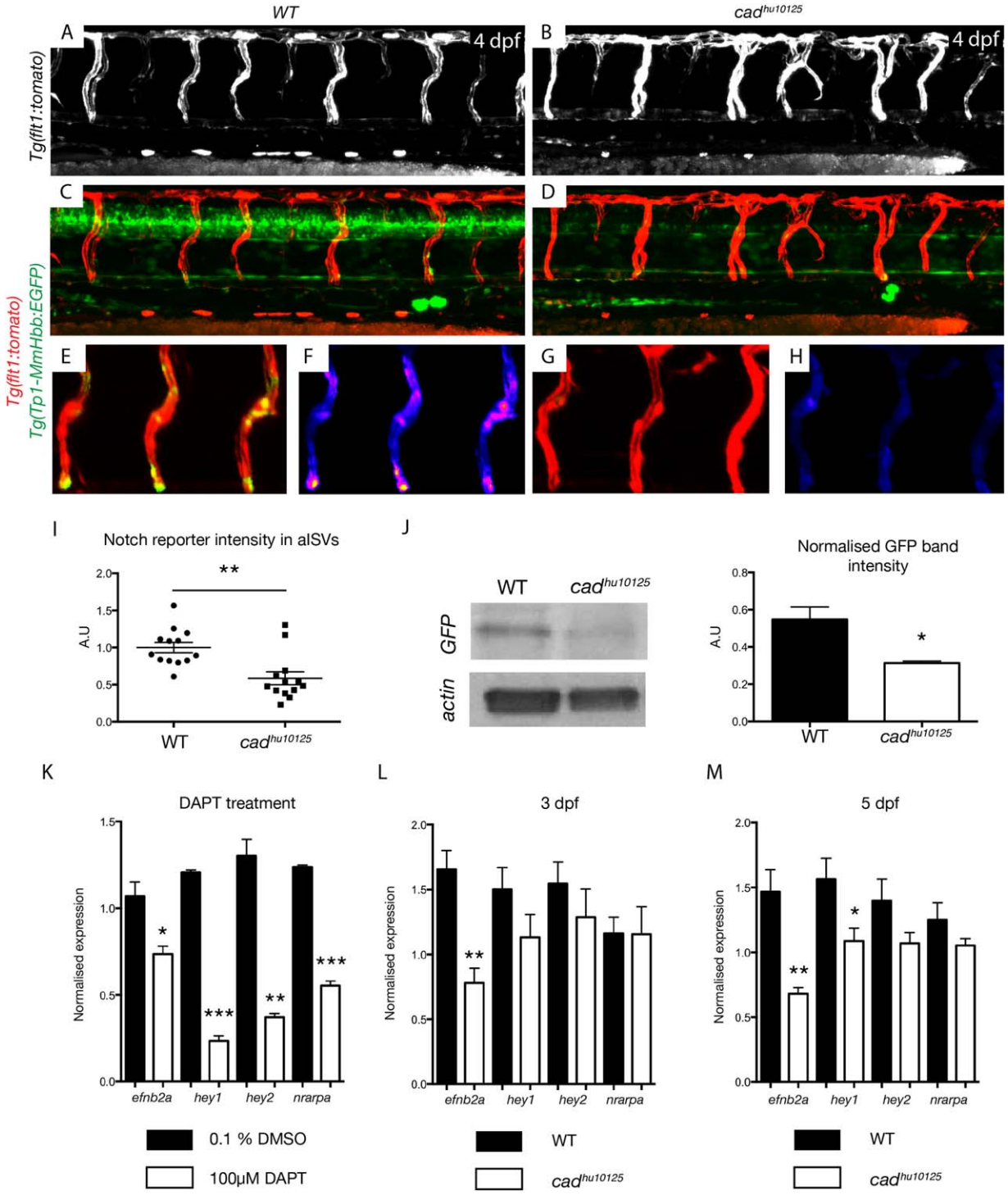


**Fig. 4.** Notch signaling is reduced in *cad*$^{hu10125}$ mutants. **A–D:** The vasculature *Tg(flt1:tomato*, *Tp1-MmHbb:EGFP)* in wild-type siblings (n = 43) and cad$^{hu10125}$ (n = 12) embryos at 4 dpf, (A,B), *Tg(flt1:tomato)*; (C,D), *Tg(Tp1-MmHbb:EGFP; flt1:tomato)*. **E–H** Computer assisted segregation of vascular specific expression of (*Tp1-MmHbb:EGFP*) in *Tg(flt1:tomato*, *Tp1-MmHbb:EGFP)* wild-type siblings (n = 13 embryos, 40 aISVs analysed) and *cad*$^{hu10125}$ (n = 13 embryos, 38 aISVs analysed) at 4 dpf. **E,G:** aISVs, *Tg(flt1:tomato*, *Tp1-MmHbb:EGFP)* positive, in wild-type siblings (E) and *cad*$^{hu10125}$ embryos (G) at 4 dpf. **F,H:** aISVs-restricted expression of Tg(*Tp1-MmHbb:EGFP)* in wild-type siblings (F) and *cad*$^{hu10125}$ embryos (H) at 4 dpf. Fluorescence intensity is displayed as a heat map, with a low to high color-coded from blue to white. **I:** Quantification of aISV-restricted Notch-reporter intensity based on analysis displayed in (F) and (H) ($P = 0.0012$). Each point represents the average aISV signal intensity in individual WT sibling embryos (n = 13 embryos, 40 aISVs analysed) or *cad*$^{hu10125}$ embryos (n = 13 embryos, 38 aISVs analysed) normalised to average WT sibling signal intensity. **J:** Western blot detection of GFP expression in 48 hpf pooled embryos from WT and *cad*$^{hu10125}$ Notch reporter transgenic embryos. The level of GFP expression is significantly reduced in *cad*$^{hu10125}$ embryos ($P = 0.0274$). The expression of actin was used to monitor protein input and normalise GFP band intensity. **K:** Quantitative RT-PCR for the Notch target genes *efnb2a*, *hey1*, *hey2*, and *nrarpa* in embryos treated with 0.1% DMSO (black columns) or 100 μM DAPT (white columns), shows that the expression of these genes is significantly reduced when Notch signaling is inhibited from 24 hpf to 3dpf) (3 biological replicates, ≥10 embryos each). **L,M:** Quantitative RT-PCR for the Notch target genes *efnb2a*, *hey1*, *hey2* and *nrarpa* in WT (black columns) and *cad*$^{hu10125}$ (white columns) embryos at 3 dpf (WT, n = 5; *cad*$^{hu10125}$, n = 5 biological replicates, ≥10 embryos each)(L) and 5 dpf (WT, n = 5; *cad*$^{hu10125}$, n = 4 biological replicates, ≥10 embryos each) (M). *efnb2a* reduction at 3 dpf, $P = 0.0017$, 5 dpf $P = 0.0082$.; *hey1* reduction at 5 dpf, $P = 0.0437$. Other trends nonsignificant in *cad*$^{hu10125}$ mutants but significant in DAPT treated embryos.

supported by numerous studies (reviewed in Haines and Irvine, 2003). The Notch receptor presents with multiple target sites for UDP-dependent glycosylation events (Haines and Irvine, 2003). These notably involve EGF repeats, which are key components of the extracellular domain of the Notch receptor (Shao et al., 2002) and crucially involved in ligand-receptor interactions. Hence, we suggest that Cad and UDP-dependent glycosylation of the Notch receptor is probably required for Notch activity and vascular development.

As *cad*$^{hu10125}$ embryos do not exhibit phenotypes equivalent to pan-Notch deficiency such as those seen in *mindbomb* mutants or early DAPT-treated embryos (Schier et al., 1996; Lawson et al., 2001; Lawson and Weinstein, 2002; Itoh and Chitnis, 2003; Leslie et al., 2007; Ozbudak and Lewis, 2008; Therapontos and Vargesson, 2010), it is likely that early Notch signaling is either supported by maternally deposited UDP or maternally deposited Cad. Consistent with this, is the progressive nature of the *cad*$^{hu10125}$ artery phenotype, with no defects at 30 hpf, mild branching phenotypes at 2 dpf but gradually more severe hyperbranching as development proceeds. This is likely observed progressively because maternally deposited Cad or UDP is continually depleted as development proceeds. The later stage hyperbranching may also suggest that Notch suppression of Vegf-responsiveness is ongoing, beyond just the process of angiogenic sprouting.

While the results presented here support the possibility that posttranslational glycosylation of Notch plays a role in the regulation of angiogenesis, we have not demonstrated actual functionally important targets of Cad-dependent modifications in vivo. It is, therefore, possible that the effect could be indirect, with other undetermined modulators of Notch activity requiring Cad or UDP. Our findings now mandate a further in-depth biochemical assessment of UDP-dependent glycosylation in this pathway. Though assessing the glycosylation state of the multiple components of the Notch pathway is technically challenging, and most knowledge in the field relies on in vitro assays (Bruckner et al., 2000; Moloney et al., 2000a,b; Panin et al., 2002), this new model may prove amenable to investigation in vivo in zebrafish, particularly in the context of angiogenesis.

Therapeutic strategies targeting angiogenic pathways have begun to move laterally toward broadly-acting cellular and metabolic pathways within endothelial cells (Bottsford-Miller et al., 2012; De Bock et al., 2013). Alternative target pathways to manipulate the Notch/Vegf axis such as Cad or UDP-biosynthetic enzymes have potential that is highlighted well by the dramatic developmental angiogenesis phenotypes described here.

## Experimental Procedures

### Zebrafish Strains

All animal use was approved by and conformed to ethical guidelines of the animal ethics committees at the University of Queensland and the Hubrecht Institute. Zebrafish were maintained using standard husbandry procedures. ENU mutagenesis was performed as previously described in (Wienholds et al., 2002). The *cad*$^{hi2694}$, *Tg(fli1a:EGFP)*$^{y1}$ referred as *Tg(fli1a:EGFP)*, *Tg(−6.5kdrl:mCherry)*$^{s916}$ referred as *Tg(kdrl:mcherry)*, *Tg(−0.8flt1:tdTomato)*$^{hu5333Tg}$ referred as *Tg(flt1:tomato)*, *Tg(EPV.Tp1-Mmu.Hbb:EGFP)*$^{um14}$ referred as *Tg(Tp1-MmHbb:EGFP)*, *Tg(fli1:nEGFP)*$^{y7}$ referred as *Tg(fli1:nucEGFP)*, and *Tg(flt1:YFP)*$^{hu4624}$ referred to as *Tg(flt1:YFP)* lines are described in (Lawson and Weinstein, 2002; Amsterdam et al., 2004; Siekmann and Lawson, 2007; Hogan et al., 2009b; Parsons et al., 2009; Bussmann et al., 2010). The *cad*$^{hi2694}$ and *tyms*$^{hi3510Tg}$ alleles were sourced through the Zebrafish International Resource Center.

### Genetic Mapping

Meiotic mapping of the *cad* mutation in *cad*$^{hu10125}$ embryos was performed using the Ensembl database (http://www.ensembl.org), release Zv9. The single sequence length polymorphism markers used were: *Z20582* (16 Mb. Zv9), *Z26487* (22.9 Mb. Zv9), *Z23654* (33.1 Mb. Zv9), *Z536* (39.1 Mb. Zv9), *Z14605* (39.9 Mb. Zv9).

### Imaging and Analysis

For live confocal imaging, embryos were mounted as previously described (Hogan et al., 2009b). Imaging was performed in the Australian Cancer Research Foundation's Dynamic Imaging Facility at the Institute for Molecular Bioscience on a LSM Zeiss 510 NLO, META, or Zeiss 710 FCS confocal microscope using $\times 10$ or $\times 20$ dry objectives. Images were acquired with the Zeiss Zen software and analyzed with Photoshop suite, Biplane IMARIS and Fiji. Biplane IMARIS software was used to limit the analysis in the *Tg(Tp1-MmHbb:EGFP)* strain to cells expressing *Tg(flt1:Tomato)* (aISVs). Quantification of aISV fluorescence intensity was performed using the Plot-profile plugin of Fiji (ImageJ 1.47), applied on Z-axis maximum intensity projection of 4 individual aISVs per embryo. The aISV-restricted fluorescence intensity of the *Tg(Tp1-MmHbb:EGFP)* reporter of both wild-type and *cad*$^{hu10125}$ mutant embryos was normalised to the average fluorescence intensity measured in wild-type sibling embryos, imaged under the same experimental settings.

### Statistical Analysis

We used unpaired student *t*-tests using Prism (Graph Pad software) for all Figures except Figure 3F, where an ANOVA was performed. *P*-values are represented in the Figures as $^{*}P \leq 0.05$, $^{**}P \leq 0.01$, $^{***}P \leq 0.001$, and $^{****}P \leq 0.0001$. Standard error of the mean is represented in error bars.

### DAPT Drug Treatment

Zebrafish embryos were exposed to DMSO and DAPT (Sigma, D5942) at 0.1% and 100 μM, respectively, in E3 medium, from 24 hpf to 3 dpf. The treatment medium was changed once a day. DAPT was stored according to manufacturer recommendations.

### Western Blot

Zebrafish embryos were lysed in RIPA buffer containing 50 mM Tris-HCl pH7.4, 1% Na-deoxycholate, 150 mM NaCl, 1 mM EDTA, 1% Triton-X 100, 0.1% SDS, 1 mM PMSF and a protease inhibitor cocktail (Sigma-Aldrich, P8340). Samples were resolved by SDS-PAGE, transferred onto PVDF membrane (BIO-RAD, 170–4272), and blotted with antibodies against mouse anti-chicken actin (EMD Millipore, MAB1501) and mouse anti-GFP (Roche, 11814460001). Western blots were developed using the ECL method (Western Blotting Analysis System, Sigma-Aldrich, RPN2109). The intensity of the bands was quantified using ImageJ (version 1.44) software.

### Whole-mount In Situ Hybridization and Immunochemistry

Zebrafish *cad* full-length cDNA was amplified as a probe template from stage mixed WT cDNA by PCR using the primers forward: 5′-cagctgcccaataacatcgc-3′ and reverse: 5′-ggatccatt aaccctcactaaagggaacgcacattgcactcgatcacc-3′. In situ hybridization was performed essentially as previously described (Thisse et al., 1993) with NBT/BCIP staining solution (Roche).

### Morpholino Oligomers

Morpholino oligomers against *vegfr3*, *vegfc*, and *ccbe1* were described in (Hogan et al., 2009a) and were injected at 5 ng per embryos. Injections were performed as described in (Hogan et al., 2008).

### Quantitative Real Time PCR Analysis

Cell isolation, RNA extraction and cDNA synthesis were performed as described in (Coxam et al., 2014). A total of 30–50 ng of amplified mRNA (FACs sorted cells) or 0.4 μg total RNA (pooled WT and $cad^{hu10125}$ mutant embryos) RNA was extracted from FACS samples from 36 and 60 hpf *Tg(flt1:YFP)*, *Tg(kdrl:mcherry)* zebrafish, with the DsRed negative/YFP positive cells corresponding to the arterial cell population.

Quantitative PCR was setup and results analysed as described in (Coxam et al., 2014).The expression of *rpl13* was used for normalisation of gene expression in the aISVs. For FAC sorted cell populations presented in Figure 2K. In WT and $cad^{hu10125}$ embryos embryos treated or not with 0.1% DMSO, 100μM DAPT (Fig. 4K–M), gene expression was normalised to the geometric average of *rpl13* and *hprt1* expression, and presented as a ratio to *cdh5* normalised expression to take into account excessive proliferation of aISVs in $cad^{hu10125}$.

The following primers were used for RT-PCR:

hey1 Fwd: 5′-CAAGCAAGAAAACGTCGCAG-3′,
hey1 Rev 5′-GTGCAGTCTCTGCTAGACATT-3′,
hey2 Fwd 5′-TGGGCAGCGAGAATAACTAC-3′,
hey2 Rev 5′-TTTTCAATGATCCCTCTCCGC-3′,
nrarpa Fwd 5′-AAGTGTGTCGTTTACTTGTCCT-3′,
nrarpa Rev 5′-TAAAACCAGTTTAGGCGCGT-3′,
ephb2a Fwd 5′-AGGAACAACCGTCCGAAATT-3′,
ephb2a Rev: 5′-GGAGAAGTCTGGTGTGCTAC-3′.

## Acknowledgments

We thank Scott Paterson, Neil Bower, and Merlijn Witte for technical assistance and advice. B.M.H. and K.A.S. were funded by ARC Future Fellowships. S.S.M. is supported by the KNAW. Imaging was performed in the Australian Cancer Research Foundation's Dynamic Imaging Facility at IMB.

## References

Adams RH, Alitalo K. 2007. Molecular regulation of angiogenesis and lymphangiogenesis. Nat Rev Mol Cell Biol 8:464–478.

Amsterdam A, Nissen RM, Sun Z, Swindell EC, Farrington S, Hopkins N. 2004. Identification of 315 genes essential for early zebrafish development. Proc Natl Acad Sci U S A 101:12792–12797.

Bahary N, Goishi K, Stuckenholz C, Weber G, Leblanc J, Schafer CA, Berman SS, Klagsbrun M, Zon LI. 2007. Duplicate VegfA genes and orthologues of the KDR receptor tyrosine kinase family mediate vascular development in the zebrafish. Blood 110:3627–3636.

Blair SS. 2000. Notch signaling: fringe really is a glycosyltransferase. Curr Biol 10:R608–R612.

Bottsford-Miller JN, Coleman RL, Sood AK. 2012. Resistance and escape from antiangiogenesis therapy: clinical implications and future strategies. J Clin Oncol 30:4026–4034.

Bruckner K, Perez L, Clausen H, Cohen S. 2000. Glycosyltransferase activity of Fringe modulates Notch-Delta interactions. Nature 406:411–415.

Bussmann J, Bos FL, Urasaki A, Kawakami K, Duckers HJ, Schulte-Merker S. 2010. Arteries provide essential guidance cues for lymphatic endothelial cells in the zebrafish trunk. Development (Cambridge, England) 137:2653–2657.

Covassin LD, Villefranc JA, Kacergis MC, Weinstein BM, Lawson ND. 2006. Distinct genetic interactions between multiple Vegf receptors are required for development of different blood vessel types in zebrafish. Proc Natl Acad Sci U S A 103:6554–6559.

Coxam B, Sabine A, Bower NI, Smith KA, Pichol-Thievend C, Skoczylas R, Astin JW, Frampton E, Jaquet M, Crosier PS, Parton RG, Harvey NL, Petrova TV, Schulte-Merker S, Francois M, Hogan BM. 2014. Pkd1 regulates lymphatic vascular morphogenesis during development. Cell Rep 7:623–633.

De Bock K, Georgiadou M, Schoors S, Kuchnio A, Wong BW, Cantelmo AR, Quaegebeur A, Ghesquiere B, Cauwenberghs S, Eelen G, Phng LK, Betz I, Tembuyser B, Brepoels K, Welti J, Geudens I, Segura I, Cruys B, Bifari F, Decimo I, Blanco R, Wyns S, Vangindertael J, Rocha S, Collins RT, Munck S, Daelemans D, Imamura H, Devlieger R, Rider M, Van Veldhoven PP, Schuit F, Bartrons R, Hofkens J, Fraisl P, Telang S, Deberardinis RJ, Schoonjans L, Vinckier S, Chesney J, Gerhardt H, Dewerchin M, Carmeliet P. 2013. Role of PFKFB3-driven glycolysis in vessel sprouting. Cell 154:651–663.

Geudens I, Herpers R, Hermans K, Segura I, Ruiz de Almodovar C, Bussmann J, De Smet F, Vandevelde W, Hogan BM, Siekmann A, Claes F, Moore JC, Pistocchi AS, Loges S, Mazzone M, Mariggi G, Bruyere F, Cotelli F, Kerjaschki D, Noel A, Foidart JM, Gerhardt H, Ny A, Langenberg T, Lawson ND, Duckers HJ, Schulte-Merker S, Carmeliet P, Dewerchin M. 2010. Role of delta-like-4/Notch in the formation and wiring of the lymphatic network in zebrafish. Arterioscler Thromb Vasc Biol 30:1695–1702.

Guruharsha KG, Kankel MW, Artavanis-Tsakonas S. 2012. The Notch signalling system: recent insights into the complexity of a conserved pathway. Nat Rev Genet 13:654–666.

Habeck H, Odenthal J, Walderich B, Maischein H, Schulte-Merker S, Tubingen screen c. 2002. Analysis of a zebrafish VEGF receptor mutant reveals specific disruption of angiogenesis. Curr Biol 12:1405–1412.

Haines N, Irvine KD. 2003. Glycosylation regulates Notch signalling. Nat Rev Mol Cell Biol 4:786–797.

Herbert SP, Stainier DY. 2011. Molecular control of endothelial cell behaviour during blood vessel morphogenesis. Nat Rev Mol Cell Biol 12:551–564.

Hogan B, Bos F, Bussmann J, Witte M, Chi N, Duckers H, Schulte-Merker S. 2009a. Ccbe1 is required for embryonic lymphangiogenesis and venous sprouting. Nat Genet 41:396–398.

Hogan B, Verkade H, Lieschke G, Heath J. 2008. Manipulation of gene expression during zebrafish embryonic development using transient approaches. Methods Mol Biol 469:273–300.

Hogan BM, Herpers R, Witte M, Helotera H, Alitalo K, Duckers HJ, Schulte-Merker S. 2009b. Vegfc/Flt4 signalling is suppressed by Dll4 in developing zebrafish intersegmental arteries. Development 136:4001–4009.

Isogai S, Lawson ND, Torrealday S, Horiguchi M, Weinstein BM. 2003. Angiogenic network formation in the developing vertebrate trunk. Development (Cambridge, England) 130:5281–5290.

Itoh M, Chitnis A. 2003. Mind bomb is a ubiquitin ligase that is essential for efficient activation of Notch signaling by Delta. FASEB J 17:A995–A995.

Itoh M, Kim CH, Palardy G, Oda T, Jiang YJ, Maust D, Yeo SY, Lorick K, Wright GJ, Ariza-McNaughton L, Weissman AM, Lewis

J, Chandrasekharappa SC, Chitnis AB. 2003. Mind bomb is a ubiquitin ligase that is essential for efficient activation of Notch signaling by Delta. Dev Cell 4:67–82.
Jeltsch M, Jha SK, Tvorogov D, Anisimov A, Leppanen VM, Holopainen T, Kivela R, Ortega S, Karpanen T, Alitalo K. 2014. CCBE1 enhances lymphangiogenesis via A disintegrin and metalloprotease with thrombospondin motifs-3-mediated vascular endothelial growth factor-C activation. Circulation 129:1962–1971.
Jones ME. 1980. Pyrimidine nucleotide biosynthesis in animals: genes, enzymes, and regulation of UMP biosynthesis. Annu Rev Biochem 49:253–279.
Kartopawiro J, Bower NI, Karnezis T, Kazenwadel J, Betterman KL, Lesieur E, Koltowska K, Astin J, Crosier P, Vermeren S, Achen MG, Stacker SA, Smith KA, Harvey NL, Francois M, Hogan BM. 2014. Arap3 is dysregulated in a mouse model of hypotrichosis-lymphedema-telangiectasia and regulates lymphatic vascular development. Hum Mol Genet 23:1286–1297.
Koltowska K, Betterman KL, Harvey NL, Hogan BM. 2013. Getting out and about: the emergence and morphogenesis of the vertebrate lymphatic vasculature. Development 140:1857–1870.
Kovall RA, Blacklow SC. 2010. Mechanistic insights into Notch receptor signaling from structural and biochemical studies. Curr Top Dev Biol 92:31–71.
Lawson ND, Scheer N, Pham VN, Kim CH, Chitnis AB, Campos-Ortega JA, Weinstein BM. 2001. Notch signaling is required for arterial-venous differentiation during embryonic vascular development. Development 128:3675–3683.
Lawson ND, Weinstein BM. 2002. In vivo imaging of embryonic vascular development using transgenic zebrafish. Dev Biol 248: 307–318.
Le Guen L, Karpanen T, Schulte D, Harris NC, Koltowska K, Roukens G, Bower NI, van Impel A, Stacker SA, Achen MG, Schulte-Merker S, Hogan BM. 2014. Ccbe1 regulates Vegfc-mediated induction of Vegfr3 signaling during embryonic lymphangiogenesis. Development 141:1239–1249.
Leslie JD, Ariza-McNaughton L, Bermange AL, McAdow R, Johnson SL, Lewis J. 2007. Endothelial signalling by the Notch ligand Delta-like 4 restricts angiogenesis. Development 134:839–844.
Moloney DJ, Panin VM, Johnston SH, Chen J, Shao L, Wilson R, Wang Y, Stanley P, Irvine KD, Haltiwanger RS, Vogt TF. 2000a. Fringe is a glycosyltransferase that modifies Notch. Nature 406:369–375.
Moloney DJ, Shair LH, Lu FM, Xia J, Locke R, Matta KL, Haltiwanger RS. 2000b. Mammalian Notch1 is modified with two unusual forms of O-linked glycosylation found on epidermal growth factor-like modules. J Biol Chem 275:9604–9611.
Nasevicius A, Larson J, Ekker SC. 2000. Distinct requirements for zebrafish angiogenesis revealed by a VEGF-A morphant. Yeast 17:294–301.
Ozbudak EM, Lewis J. 2008. Notch signalling synchronizes the zebrafish segmentation clock but is not needed to create somite boundaries. PLoS Genet 4:e15.
Panin VM, Shao L, Lei L, Moloney DJ, Irvine KD, Haltiwanger RS. 2002. Notch ligands are substrates for protein O-fucosyltransferase-1 and Fringe. J Biol Chem 277:29945–29952.
Parsons MJ, Pisharath H, Yusuff S, Moore JC, Siekmann AF, Lawson N, Leach SD. 2009. Notch-responsive cells initiate the secondary transition in larval zebrafish pancreas. Mech Dev 126: 898–912.
Schier AF, Neuhauss SC, Harvey M, Malicki J, Solnica-Krezel L, Stainier DY, Zwartkruis F, Abdelilah S, Stemple DL, Rangini Z, Yang H, Driever W. 1996. Mutations affecting the development of the embryonic zebrafish brain. Development 123:165–178.
Shao L, Luo Y, Moloney DJ, Haltiwanger R. 2002. O-glycosylation of EGF repeats: identification and initial characterization of a UDP-glucose: protein O-glucosyltransferase. Glycobiology 12: 763–770.
Siekmann AF, Lawson ND. 2007. Notch signalling limits angiogenic cell behaviour in developing zebrafish arteries. Nature 445:781–784.
Therapontos C, Vargesson N. 2010. Zebrafish notch signalling pathway mutants exhibit trunk vessel patterning anomalies that are secondary to somite misregulation. Dev Dyn 239:2761–2768.
Thisse C, Thisse B, Schilling TF, Postlethwait JH. 1993. Structure of the zebrafish snail1 gene and its expression in wild-type, spadetail and no tail mutant embryos. Development 119:1203–1215.
Villefranc JA, Nicoli S, Bentley K, Jeltsch M, Zarkada G, Moore JC, Gerhardt H, Alitalo K, Lawson ND. 2013. A truncation allele in vascular endothelial growth factor c reveals distinct modes of signaling during lymphatic and vascular development. Development 140:1497–1506.
Wienholds E, Schulte-Merker S, Walderich B, Plasterk RH. 2002. Target-selected inactivation of the zebrafish rag1 gene. Science 297:99–102.
Willer GB, Lee VM, Gregg RG, Link BA. 2005. Analysis of the Zebrafish perplexed mutation reveals tissue-specific roles for de novo pyrimidine synthesis during development. Genetics 170: 1827–1837.
Yeh E, Dermer M, Commisso C, Zhou L, McGlade CJ, Boulianne GL. 2001. Neuralized functions as an E3 ubiquitin ligase during Drosophila development. Curr Biol 11:1675–1679.